DBN-Based MPPT Algorithm with FOPID Control for Optimal Power Tracking, Reliability, and Efficiency in Solar PV Systems under Shaded Conditions

Indexed by:
Web of Science Group

Jenifer Suriya L J[a,*], Christy Mano Raj J S[b]

[a] Department of Electronics and Communication Engineering, Loyola- ICAM College of Engineering and Technology, Chennai, India
[b] Department of Electrical and Electronics Engineering, Government College of Engineering, Bargur, India

Highlights

- Utilizing a grid integration model.
- Proposed intelligent MPP is utilized to locate the overall MPP.
- Utilizing the Green Anaconda Optimization based DBN.
- Increase efficiency and reducing harmonics.

Abstract

Monitoring the Maximum Power Point Tracking (MPPT) is one among the most crucial jobs in a solar system. Significant issues with solar power generation, including the installation and operation of PV panels, include harmonic distortion and electromagnetic radiation interference. As a result, the MPPT controller in the proposed work utilizes deep learning to track the MPP. Developing a Deep Belief Network (DBN) using the generated dataset allows it to determine the MPPT. Utilizing the Green Anaconda Optimization (GAO) based DBN to provide the reference or attained voltage, the fractional order controller is then used to generate the converter's pulse. The suggested methods outperform prior MPPT methods in terms of steady state response, oscillation-free operation, loss reduction, and time to settle down at MPP. The suggested model provides very low harmonic values, such as 0.78% for voltage THD and 0.781% for current THD, and accuracy of 99.8%. The outcomes show that, the optimal DBN MPPT approach works better than the controllers.

Keywords

deep belief network, FOPID controller, green anaconda optimization, PV panels, maximum power point tracking, power efficiency.

1. Introduction

It is anticipated that in the next years, energy demand would continue to rise significantly at a rate that has been steadily rising [1]. Geothermal, solar, wind, and tidal energy sources are among the rapidly developing renewable energy sources that help reduce the use of fossil fuels and protect the ecosystem from pollutants. The most popular energy source, aside from wind power, is solar energy, which holds a significant share of the market in the worldwide energy industry [2]. To improve system performance, in addition to refining PV module production processes and converter power electronics, an effective MPPT controller has to be used to increase system flow [3]. When the temperature and solar radiation conditions vary broadly the MPPT algorithm works in combination with an inverter or DC/DC converter to ensure that the MPP can consistently achieve the goal [4].

As a result of their ease of use and simplicity, the traditional MPPT approaches have been widely adopted [5]. Their main flaw is that, in Partial Shadowing Conditions (PSCs), they can't

(*) Corresponding author.
E-mail addresses: Jenifer Suriya L J, (ORCID: 0009-0001-5138-4783) jenifersuriya.lj@licet.ac.in, Christy Mano Raj J S (ORCID: 0000-0003-2972-2026) christymanoraj@gcebargur.ac.in,

get out of their captivity at a nearby MPP, which results at limited energy adaptation [6]. In an attempt to address the P&O method's shortcomings of poor convergence, high oscillation, and slow tracking speed [7]. In this case, if the MPP stays farther away, the controller has the option of selecting a large step size. The purpose of the short step size is to reduce instability as it gets closer to the MPP [8]. Kumar and Shivashankar [17] recommend carrying out research to improve modeling and control strategies for a grid-connected HWSES. Akram et al. [18] developed the Firefly Algorithm (FA), a meta-heuristic optimization-based method for determining a solar photovoltaic system's MPP and analysing Partial Shadowing Conditions (PSC). Manna et al. [19] introduces a progressive adaptive control architecture that effectively manages uncertainty and disruptions in the PV system and its environment, simplifies system control, and improves MPPT performance.

Manoharan et al. [20] recommended a variance in the PV module's output voltage, power, and current (dI) all contribute to an improved method. Xu et al. [21] present the goal of a new MPPT method is to improve response time. There are two phases to it: the computing phase and the regulating phase. Obukhov et al. [22] introduces an uncommon method for choosing the parameters of the key parts of an independent photovoltaic system with an MPPT controller, ensuring the most effective utilization of the solar energy that is available. Chalok et al. [23] develops an MPPT that is based on the fuzzy logic method. There has been numerous discussions regarding the PV array's mathematical model. Patra et al. [24] created an optimization approach in order to maximize the output power of the PV module power and constraints to perform a new planned intention role simultaneously. González-Castaño et al. [25] developed a fast-tracking hybrid MPPT technique based on Surface-Based Polynomial Fitting and P&O has been presented for solar PV under PSCs. Dagal et al. [26] presented the hybridization of the SSA with Particle Swarm Optimization (PSO) for MPPT of PV systems that are optimal.

Sivakumar et al. [27] developed a Better solutions are still being developed, and it has been strongly recommended to follow international standards. As a result, this article proposes microgrid clusters that are powered by renewable energy sources and integrate multiple structures in an urban environment. By controlling the available energy within the cluster rather of concentrating it around the utility grid, this improves the reliability of the power sources.

Adam Rasid et al. [28] developed a how photovoltaic (PV) systems are affected by shading. This study details the PV system that was put in place on the roof of the Polytechnic State of Ujung Pandang-Makassar, Indonesia, administration building (PNUP). The shading impact, loss diagram, and performance ratio (PR) were assessed throughout the year using the PVsyst program in order to implement the suggested approach.

Chakarajamula et al. [29] developed the solar natural source is selected for generating the electricity. Due to the nonlinear behavior of PV, achieving maximum voltage from the Photovoltaic (PV) system is a more tough job. In this work, various hybrid optimization controllers are studied for tracing the working power point of the PV under different Partial Shading Conditions.

Lixin Zhang et al. [30] developed partial shading conditions cause the output of PV systems to exhibit nonlinear and multipeak characteristics, resulting in a loss of output power. In this paper, we propose a novel Maximum Power Point Tracking (MPPT) technique for PV systems based on the Dung Beetle Optimization Algorithm to maximize the output power of PV systems under various weather conditions.

Abdulbari Talib et al. [31] developed the effective harnessing of maximum solar energy in photovoltaic (PV) systems faces a significant challenge due to weather fluctuations. This challenge becomes particularly pronounced for PV systems aiming to achieve optimal power output during Maximum Power Point Tracking (MPPT), especially under partial shading conditions.

From the aforementioned related study, MPPT can be used to increase a PV system's power efficiency in any circumstance. Even these current techniques have certain shortcomings, such as underfitting or overfitting the neural model [26], transient responses and stability [17], computational complexity [24], [25], implementation costs and less tracking efficiency [18] [19] [21] [22], conventional method is not appropriate [23] and limited durability [20]. To address these shortcomings, a sophisticated intelligent controller technique is created to improve a PV integrated system's power efficiency. In the next section, a brief explanation of the suggested method procedure

and its numerical investigations are provided.

Another form of MPPT control created is based on soft computing techniques, such as fuzzy logic control (FLC) [9], support vector machine, ANN [10], and ANFIS [11]. Though, according to the evolution algorithms, specific methods like the Genetic optimization [12], Cuckoo Search optimization [13], Ant Colony Optimization [14], Bee Colony optimization [15], and bio-inspired memetic salp swarm algorithm [16], etc., are recommended. For reduced computing time, a costly microprocessor is typically needed, and for low convergence randomness, expertise in a specific PV system. To solve this issue the suggested model employs an optimal DBN to regulate the MPPT and enhance the training procedure. The proposed model's primary contribution is outlined as follows:

- Utilizing a grid integration model, a 6kW solar system was developed to analyse power efficiency under various conditions.
- A standard dataset was created which includes temperature, voltage, current, and irradiance under various conditions.
- Utilizing this dataset to design the GAO-DBN tracking system which analyses the input parameters to generate a DC-DC converter pulse signal.
- Proposed intelligent MPP is utilized to locate the overall MPP using chosen PV system data.
- Increase efficiency and reducing harmonics, create the

precise duty cycle to turn the converter ON/OFF while sending power from solar panels to the load.

The section of the manuscript is structured as follows: In section 1, a few recent studies that are pertinent to the best MPPT tracking for a system are reviewed. The proposed work's general design and methodology are presented in Section 2. The performance validation of the proposed model is shown in Section 3. Finally, section 4 offers the work's ultimate conclusion.

2. Proposed Methodology

A PV system efficiently decreases the use of fossil fuels that contribute to environmental degradation by converting solar power into electricity. To ensure that PV systems perform efficiently at the MPP in a number of weather situations, new materials for solar cells have also been introduced to boost energy conversion efficiency. These materials are known as MPPT algorithms. The traditional MPPT methods have disadvantages due to the computation time and tracking error. The proposed research developed an optimum boost converter based on a Deep Belief Network (DBN) power tracker to enhance the power supply for load power balancing. Optimally improve the DBN's learning rate to make a correct pulse to manage the power flows. The working process of the proposed MPPT power tracking is demonstrated in Figure 1.
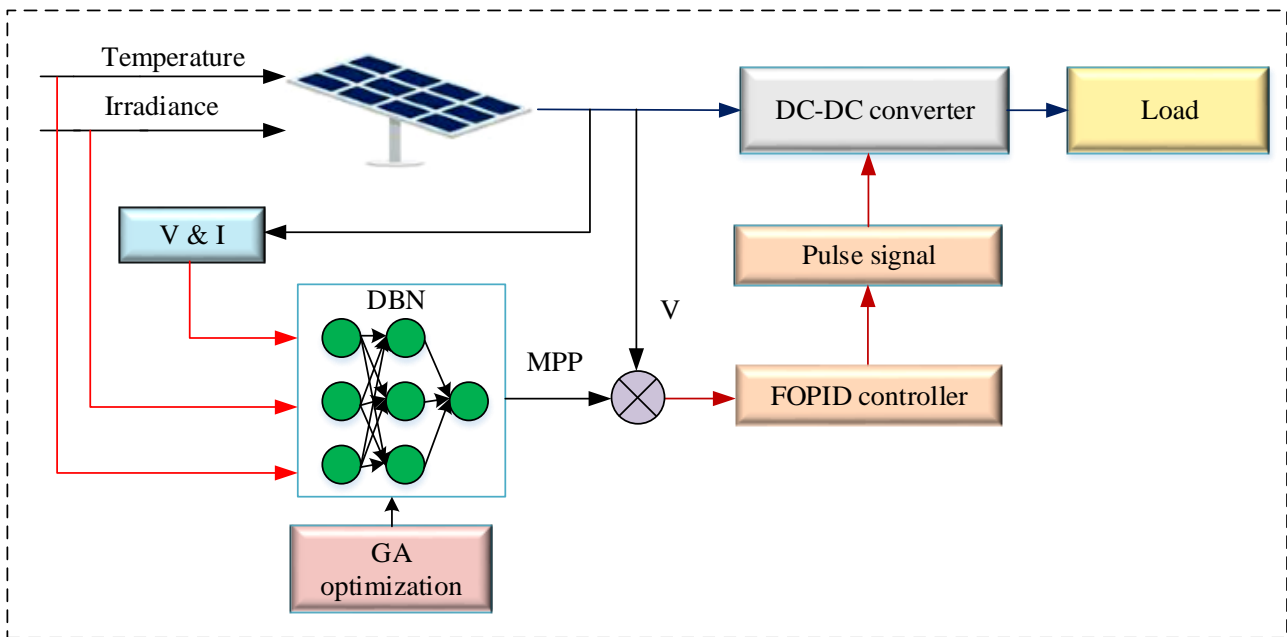

Figure 1. Schematic model of proposed optimal tracking system.

A standard PV module was designed as per the ranges, which power was irregular due to variations of temperature and irradiance, thus causing power variation. Thus, an optimal DBN tracker system based on Green Anaconda Optimization (GAO) was developed in order to track the maximum power and produce a DC-DC converter pulse signal. The tracker system was designed as per the generated dataset using the designed Simulink model. Based on the trained value the proposed tracker was operated to control the converter. The FOPID controller output was passed to the DC-DC boost converter which switching pulses are generated and provide power flow to the load. The performance of the suggested model was examined in numerous types of natural scenarios, including normal, partially and fully shading. The proposed optimal DBN tacking system-based PV models' mathematical configuration was presented in the upcoming section.

2.1. Mathematical Model of PV Module

When simulating a PV system, it's essential to employ a reliable solar cell model. Fast computation and highly accurate models are not mutually exclusive. Double-diode and single-diode PV models are the two different varieties. Despite being less accurate than the other model, the single-diode model is nonetheless chosen because of its ease of use. This study makes use of a single-diode model's solar cell equivalent electrical circuit. Kirchhoff's law states that the ideal cell's output current is provided by

$$I = I_{ph} - I_d - I_{sh} \tag{1}$$

Where the parallel resistance current, denoted as I_{sh}, is provided by

$$I_{sh} = \frac{V + IR_s}{R_p} \tag{2}$$

Where R_p is the resistance in parallel, and R_s is the resistance in series. The electrically generated current, or I_{ph}, is also proportional to the intensity of the light. It is computed using

$$I_{ph} = [I_{sc} + K_I(T_c - T_r)] \times \frac{G}{G_{STC}} \tag{3}$$

Where K_I is the cell short-circuit current temperature coefficient and I_{sc} is the short-circuit current at standard testing conditions. The temperature at which the cell operates is T_c, the reference temperature is T_r, and the irradiation is G. I_d is determined by,

$$I_d = I_0 \left[exp\left(\frac{qV_d}{AkT_c}\right) - 1 \right] \tag{4}$$

Where A is the diode's optimal factor, $k = 1.38 \times 10^{-23}$ is the Boltzmann's constant, and $q = 1.6 \times 10^{-19}$ is the electronic charge. V_d is the voltage of the analogous diode, and I_0 is the diode's reverse saturation current. They are computed using

$$V_d = V + IR_s \tag{5}$$

To develop a PV module, PV cells are typically connected in series. The photovoltaic module's current, which is simultaneously influenced by temperature and sunlight, can be calculated using the following simple mathematical model:

$$I_{pv} = I_{ph} - I_0 \left[exp\left(\frac{q(V+IR_s)}{AkT_cN_s}\right) - 1 \right] \tag{6}$$

Where N_s is the total number of resistance cells in series. Environmental conditions have a significant impact on a photovoltaic module's characteristics, as illustrated by the equation above.

2.2. Effect of partial shading condition

PV strings operate in parallel to provide with high current while attaining a specific power. To achieve the necessary voltage, a particular number of PV modules are connected in series to make each string. Under normal circumstances, the usual P-V curve shows a single MPP when all of the strings PV receive an equal irradiance. Hot-spot heating results from the shaded modules reduced ability to produce current compared to the unshaded modules when partial shading occurs in one of the PV array's modules. This disadvantage is addressed by employing an external bypass diode, which conducts each time the solar cell is reverse biased, enabling the external flow of unshaded cell current to the shaded cell.

2.3. Effect of fully shading condition

Using fully shade is a good approach to limit the amount of unwanted sunlight that enters a facility through the windows, especially in direct sunlight. Static shading is possible in both vertical and horizontal orientations. The building's orientation, scale, position, and window features all have an impact on design. It is recommended to apply horizontal shadow since sunlight falls from high solar altitudes toward the south. On the east and west, it is essential to use vertical shading in conjunction with horizontal elements. On the other hand, including a sophisticated converter increases power generation

efficiency under fully shadowing conditions.

By modifying the temperature and irradiation levels while using fully and partial shading as per the real-time analysis, the modified MPPT approach is utilized in the proposed approach.

2.4. MPPT Algorithms for Various Shaded PV Systems

A more accurate MPPT process is needed to continuously and optimally extract power under normal, fully and partially shaded conditions because conventional algorithms typically fail to optimally amend the MPP for a PV array suffering from PS. As a result, its usefulness rapidly diminishes. In the proposed model DBN based maximum power tracking is done by using GA optimization.

2.4.1. DBN MPPT Control

A neural network called a DBN, which is commonly utilized in deep learning techniques, is composed of various RBM models and traditionally uses RBMs as its components. Data features should not be captured in RBM with a single hidden layer. A different RBM network can use the features that were discovered after training it. As a result, the learning features of the entire training model are transformed into the characteristics of the final RBM network. This form of layer-wise learning results in DBN. This method can be used to extract the features of the DBN input data. The logistic regression layer is the result of the DBN, which is formed up of layered RBM models. In DBN networks, the pre-training process takes the form of alternate sampling and greedy layer-wise. Every DBN in the greedy layer as well as an RBM model are pre-trained using alternative sampling. The output produced by DBN is shown in Figure 2,
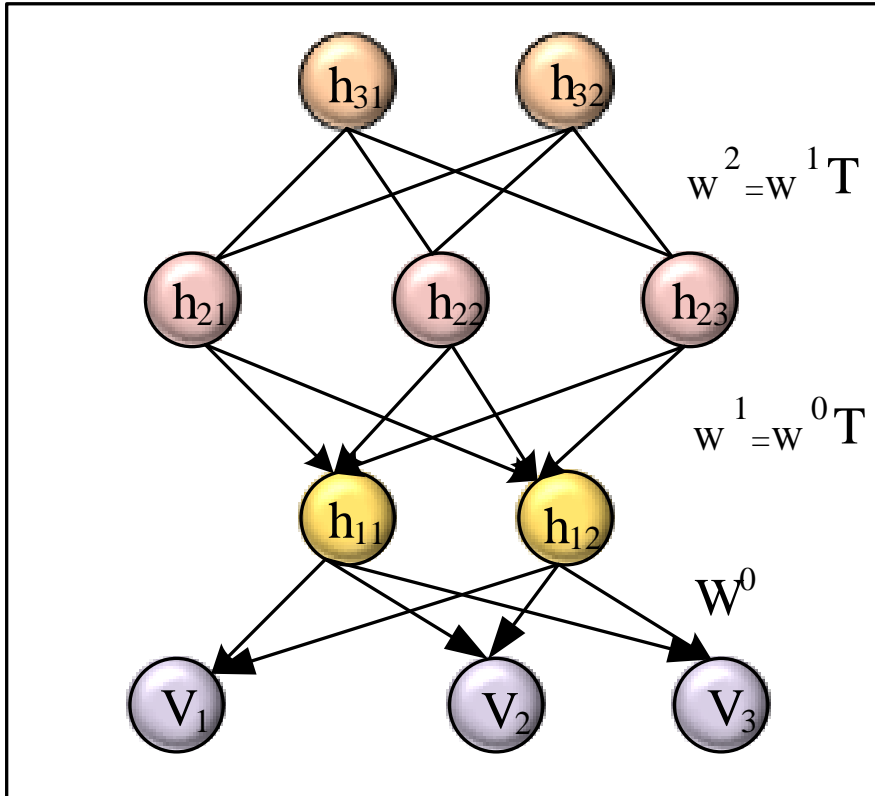

Figure 2. Process flow of DBN.

$$G_n^2 = \omega[\varpi_n^2 + \sum_m N_m^2 \times \omega_{nn}^2] \forall N_m^2 \approx G_n^1 \qquad (7)$$

G_n^2 Represents hidden neurons corresponding to RBM layers; ω_{nn}^2 combines the RBM layers hidden neuron n with visible neuron n; weight corresponding to the hidden neuron n is ϖ_n^2; N_m^2 indicates the j th input neuron; G_n^1 is hidden neuron of g of RBM. The primary disadvantage of DBN is that it may require a lot of processing and memory capacity to train effectively, in particular in complicated environments. To overcome this DBN classifier's learning rate is increased by using Green Anaconda to find the best possible solution. The manner in which the green anaconda feeds provides inspiration for it. Because of its increased robustness, it can accurately locate objects, control MPPT, and solve any optimal problem.

2.4.2. Green Anaconda Optimization

Numerous names for the South American species of boa, Eunectes murinus, commonly known as the green anaconda, including sucuri, massive anaconda, common water boa, and common anaconda. Like other boas, the green anaconda is a non-venomous constrictor and one of the longest and heaviest snakes in the world. There have been reports that green anacondas can reach a length of $5.21\ m$. Male species average $3\ m$ in length, and female species average $4.6\ m$, which makes them significantly larger. According to reports, green anacondas weigh anywhere from 30 to 70 kg. The olive-green tint of green anacondas is complemented by black spots all over their bodies. Their orange-yellow striping highlights their narrower head in relation to their larger body size. A green anaconda can swim through the water and surface due to the eyeballs on its head, covering its body. Green anacondas may eat prey that is larger than their heads because of their flexible jaw bones [21].

2.5. Steps involved in GAO

This section provides an explanation of the theory of the suggested green anaconda optimization (GAO) strategy, as well as a mathematical presentation of its modelling for use in optimization tuning.

Initialization: This initial phase involves the initialization of a set of inputs as well as the learning rate distributed including the DBN classifier.

$$L = L_1, L_2, \dots, L_n \tag{8}$$
$$N = N_1, N_2, \dots, N_n \tag{9}$$

Where, n denotes the number of population sets. In each solution set the error value is computed, based on that the fitness is evaluated.

Objective Function: The major goal is to increase resource efficiency for suppliers of cloud services. In this work, objectives are considered as loss function. Through the use of these functions as objective functions, the system's performance can be improved. The objective function is computed using the formula below:

$$fitness = 1 - loss\ function \tag{10}$$

Updation: To determine the best optimal value, the value of each iteration is updated. Green anacondas' original location in the search space has been altered by the GAO design to allow for exploration and exploitation while the search is underway.

Based on a two-phase simulation of green anaconda activity, this modification was made. The update formula was stated as follows during the exploration phase:

$$x_{i,d}^{P1} = x_{i,d} + r_{i,d} \cdot \left(SF_d^i - I_{i,d} \cdot x_{i,d}\right), i = 1,2,\dots,N\ and\ d = 1,2,\dots,m \tag{11}$$

$$X_i = \begin{cases} X_i^{P1}, & F_i^{P1} < F_i \\ X_i, & else \end{cases} \tag{12}$$

Where N is the total number of green anacondas, SF_d^i is the dth dimension of the selected female for the ith green anaconda, F_i^{P1} is the objective function value, and m is the number of possible variables. Random values with a normal distribution occur inside the interval $[0,1]$. Furthermore, $x_{i,d}^{P1}$ represents the new proposed location of the ith green anaconda based on the first phase of GAO, and $I_{i,d}$ are random values from the set $\{1,2\}$.

In the exploitation phase, the updating expression was stated as,

$$x_{i,d}^{P2} = x_{i,d} + \left(1 - 2r_{i,d}\right)\frac{ub_d - lb_d}{t}, i = 1,2,\dots,N;\ d = 1,2,\dots,m;\ and\ t = 1,2,\dots,T \tag{13}$$

$$X_i = \begin{cases} X_i^{P2}, & F_i^{P2} < F_i \\ X_i, & else \end{cases} \tag{14}$$

With respect to the second phase of GrAO, the suggested altered position of the ith green anaconda is denoted by F_i^{P2}, where $x_{i,d}^{P2}$ is the objective function value. T denotes the maximum number of iterations, P2 denotes its dth dimension, and t stands for the iteration counter.

Termination: After the optimal solution has been determined, this is the final step. Using this approach to detect the learning rate components in DQN for an effective maximum energy prediction process.

2.6. FOPID controller

For performance optimization, the FOPID controller is proposed in place of the PID controller. In addition to K_P, K_I, and K_D, two further elements in FOPID the sequence of the differentiator and the integrator offer additional chances for controller development. Fractional-order differential equation (15) provides a description of the FOPID controller.

$$u(t) = K_P e(t) + K_I D^{-\lambda} e(t) + K_D D^{\mu}\ e(t) \tag{15}$$

Where, μ signifies differential order, λ denotes integral order, both μ and λ are positive real numbers, K_D represent differential gain, K_P signifies proportional gain and K_I states

integral gain. The advantage of using this controller is that it performs better and is more flexible than a regular controller. The FOPID controller's tuning was still gets challenging. Select the optimal value for the controller parameters like $\mu, \lambda, K_D, K_I, K_P$ to provide a steady and reliable operation.

2.7. DC-DC boost converter

PV systems use DC-DC converters to control the voltage that the PV modules output. In grid-connected mode, DC-DC boost converters are utilized to increase the module voltage. One diode and one n-channel MOSFET make up the boost converter's two energy storage components. A diode and a MOSFET complement another throughout the switching operation; specifically, when a MOSFET is OFF, a diode is ON, and vice versa when a diode is OFF, a MOSFET is ON at that very moment. The boost converter's inductor and capacitor form the foundation for mathematical modelling. The inductor voltage and capacitor current can be determined in equations (16) and (17), respectively.

$$v_L = L \frac{di_L}{dt} \tag{16}$$

$$i_c = c \frac{dv_c}{dt} \tag{17}$$

Inductor V_L is depicted below for switching between OFF and ON conditions.

$$v_L = v_{in} * PWM \tag{18}$$
$$v_L = (v_{in} - v_{out}) * \overline{PWM} \tag{19}$$

Duty cycle is the ratio of $V_0 - V_{in}$ to V_0 in equation (19).

$$PWM = \frac{(v_o - v_{in})}{v_0} f_{PWM}{}^{-1} \tag{20}$$

Current passing through the inductor is computed as,

$$i_L = \frac{1}{L} \int v_L \, dt \tag{21}$$

The current and voltage through the capacitor be computed as,

$$i_C = i_L - i_R \tag{22}$$

$$v_C = \frac{1}{C} \int i_C \, dt \tag{23}$$

Following the discovery of i_C, the capacitor voltage can be calculated in Eqn. (23), which, in the case of an ideal model, yields the boost converter's load voltage.

2.8. Load

The term load refers to the object using electrical energy. Stated differently, an electrical load can be defined as a device that uses electrical energy, specifically current, and converts it into another form. Loads are classified as linear and non-linear loads.

3. Result and Discussion

In a load-connected photovoltaic system, the suggested optimal DBN controller based MPPT is utilized to enhance the power quality under all atmospheric circumstances. The suggested method is modeled in three stages: first, a basic PV model with the accompanying MPPT is created; next, a dataset is created, and finally, an optimized DBN tracker is created using that dataset. MATLAB 2021b/Simulink is used to validate the design and performance of the suggested technique. A PV array with a load connection is the first model that has been suggested. The PV array block from the MATLAB library is used to develop an array of PV modules in this case. The array's modules are linked together in parallel strings, with a series of linked modules in each string.

3.1. Dataset description

The creation of the dataset started after the PV with load-connected system was modelled. The suggested design is used in the proposed effort to build the real-time dataset. Run the simulation model first with an irradiation level of 200 and a temperature of 20 degrees. A dataset is produced by adjusting the temperature and irradiance from 20 to 25 degrees and 200 to 1000, respectively.

Table 1. Simulation Parameter with its Ranges.

Parameter	Model	Ranges
Power		6000W
No of cells		4
Resistance 1		0.005*10
Resistance 2	PV	100
Ron		5995.5
Rs		500
Cs		250 e-9
Nominal phase voltage		1000
Frequency		60
Active power	Load	10 e3
QL		100
QC		100
RS	DC-DC converter	2500
Ron		1 e-9

The simulation is carried out 200 times in total. The big temperature values in the dataset reflect the fact that, under actual meteorological circumstances, there may be

a significant variation between the highest and lowest temperatures for a certain geographic area. Table 1, demonstrates the overall simulation parameter of the proposed model. The dataset is created and then used as the basis for designing a DBN. The GAO algorithm enhances the MPPT tracker's performance by selecting the optimal value of weight and learning rates. Temperature, voltage, the equivalent amount of solar radiation and current are fed into the controller as inputs. Maximum voltage, also known as reference voltage, is the output. To determine the FOPID controller, the PV voltage and MPPT voltage are measured and compared. The FOPID controller minimizes error to generate a modified DC-DC converter pulse signal. Power quality is enhanced by producing an adequate pulse signal from the redesigned converter. Reducing the inrush current and balancing the source and load impedances are the two goals of employing the redesigned converter. The duty ratio controls the flow of power by varying the duty cycle ON/OFF. The percentage of time that an electronic equipment is turned on is known as the duty ratio, and it can be stated as a percentage or a ratio. To achieve the desired value, the MPP increases by a small percentage. To meet the demand of the consumer load, the grid system receives error-free current. Table 2, demonstrates the parameter values of the DBN tracking based pulse generation system.

Table 2. Control Strategy Parameter Values.

Parameter	Component	Values
KP		0.1
KI		0.5
KD	FOPID	0.8
λ		1
μ		0.82
Transfer function		Sigmoid
Hidden layer	DBN	7
Batch size		5
Dimension		2
Max. iteration	GAO	1000
Search agent		30

The performance of the proposed framework was verified in various types of atmospheric scenarios, including normal, static and dynamic shading. These conditions are modified in accordance with the examination of values and processes in real-time.

3.2. Scenario 1: Normal atmospheric conditions

(a)

(b)
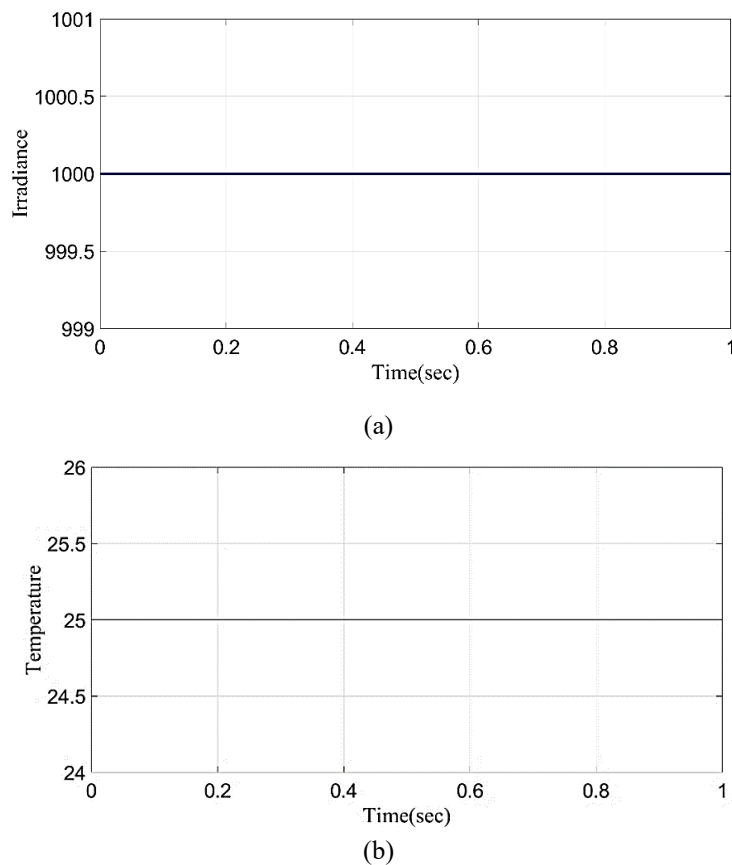
Figure 3. Evaluation of PV under normal conditions: (a) irradiance (b) temperature.

Typically, the irradiance and temperature are set to 1000 W/m^2 and 25°C, respectively in normal conditions as exposed in Figure 3. PV system's output power in this instance is $0.6 \times 10^4 W$. Similarly, the voltage is 1750V and the MPPT current is 4.5A.
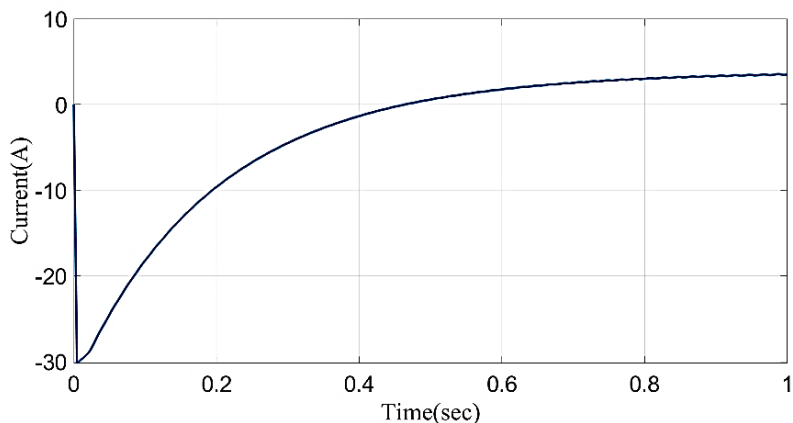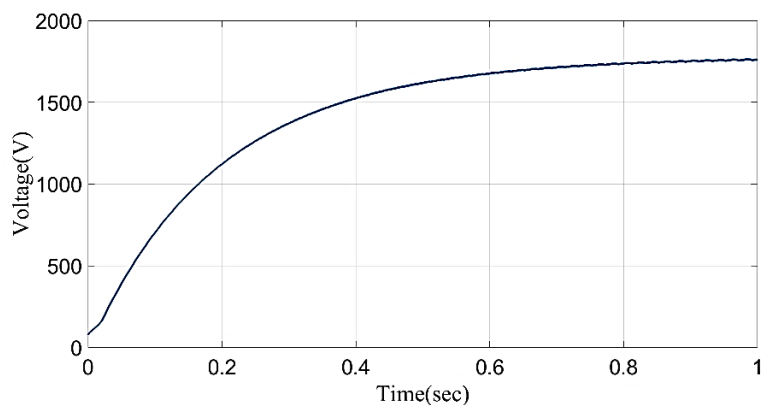
Figure 4. PV analysis under normal conditions: (a) current (b) voltage.

Figure 4, shows PV voltage and current under normal circumstances. The output in this case remained steady at 1750V and 4.5A since neither the temperature nor the amount of irradiation changed. At first, the current increases gradually until it reaches 4.3A after 0.9 seconds. After that, it flows continuously for a short while. It flowed steadily until the temperature and radiation changed from 25°C to 1000 W/m^2, at which point it reached 4.5A in 0.9 $seconds$.
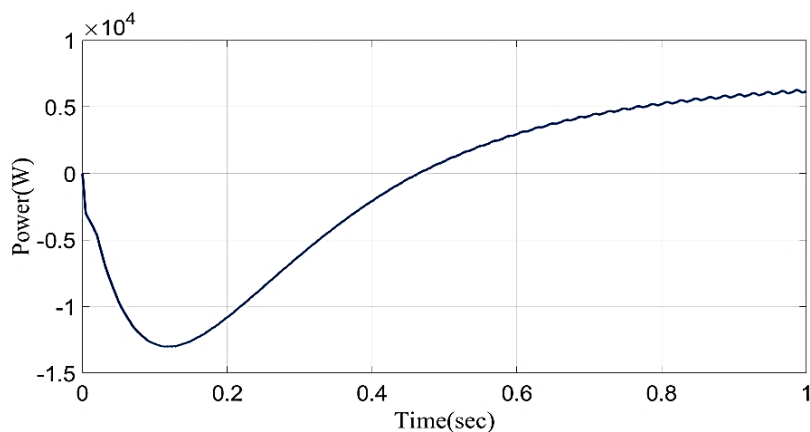
Figure 5. Analysis of PV power at normal condition.

Figure 5, illustrates the power output from the PV. PV radiation is present at a level of $1000 \, W/m^2$. The output power is $0.6 \times 10^4 W$ at that time. Under these circumstances, the MPPT voltage is 1750V. To provide the inverter with the generated constant power during this period, the optimum tracker generates a normal pulse for the boost converter.

Fundamental (50Hz) = 1827 , THD= 0.71%

(a)

Fundamental (50Hz) = 18.27 , THD= 0.72%
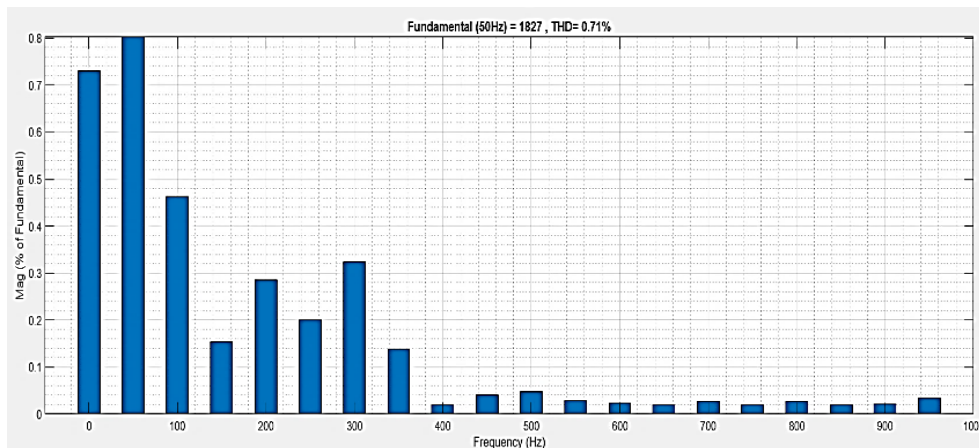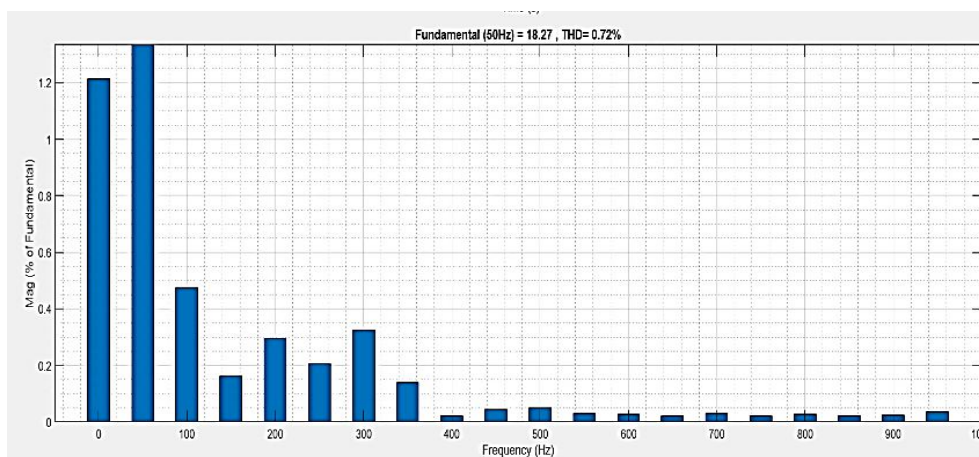
(b)

Figure 6. Harmonic analysis under typical conditions for voltage, current THD, and harmonics.

The suggested converter increases the power factor to 1 PF and has an exceptionally low Total Harmonic Distortion (THD) rating. This has a very low THD value and a very high PF when compared to other existing techniques. The voltage THD is 0.71% and the current THD is 0.72% throughout this time as clearly shown in Figure 6.
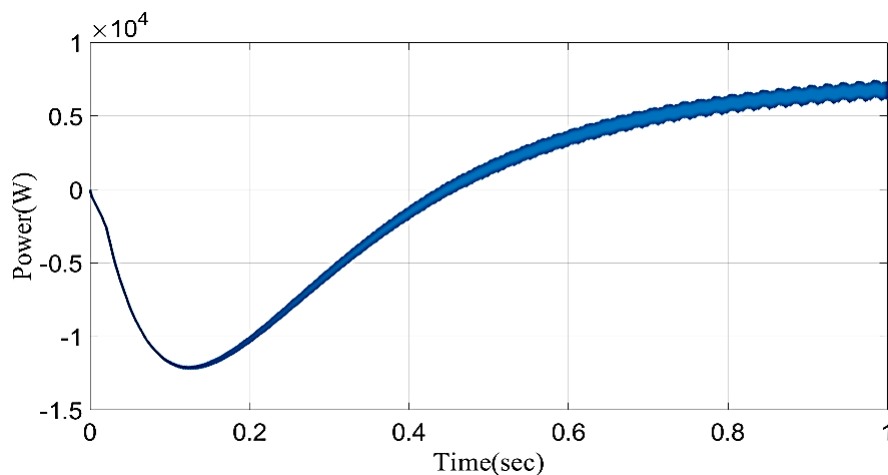
Figure 7. Analysis of DC-DC power at normal condition.

DC/DC power supplies are primarily used to generate a regulated voltage output for solar cells under a range of operating situations. Figure 7, clearly shows the DC/DC power maintains at 0.6×10^4 in normal condition.
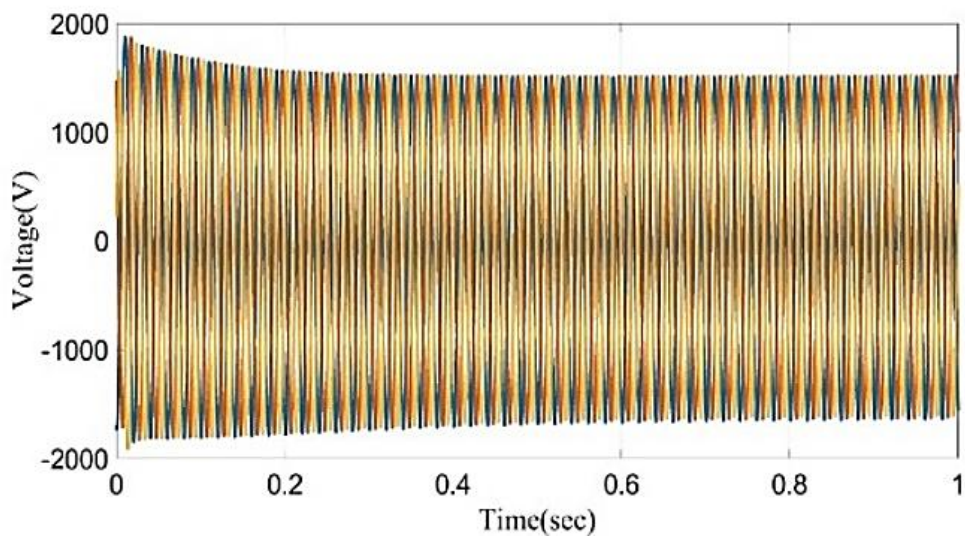
(a)
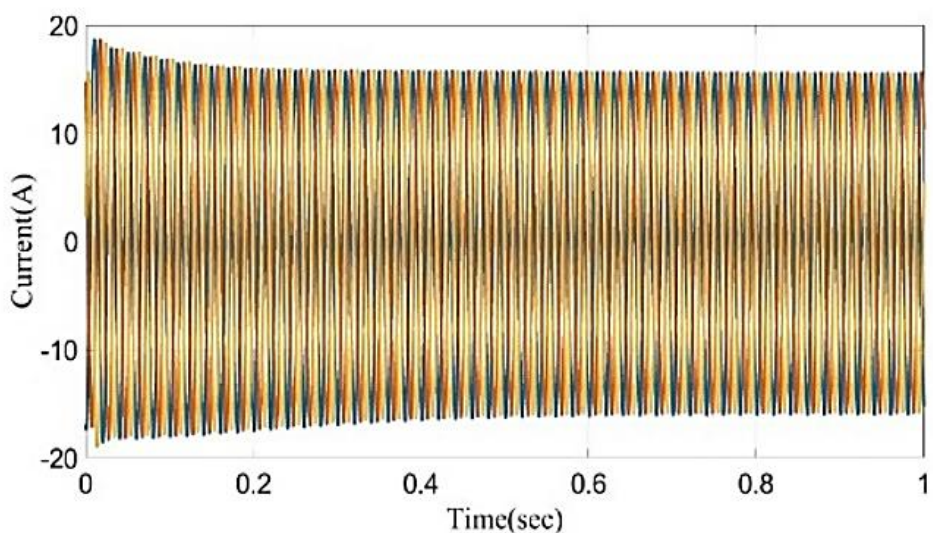
(b)

Figure 8. Examination of load voltage and load current under typical circumstances.

When a device is employed in a system, its power consumption is referred to as load. Figure 8, illustrates the load voltage and load current investigation in detail. Over 0.4 to 1 second, the load voltage is continuously maintained at 1500V. It requires between 0.2 to 1 seconds to sustain a constant 17A load current.

3.3. Scenario 2: Fully shading condition

One effective way to reduce the quantity of unwanted sunlight that reaches a building through its windows, particularly during direct sunshine, is to use static shade. It is feasible to use static shading in both horizontal and vertical orientations. The design is influenced by the building's orientation, scale, location, and window characteristics. Horizontal shadowing is advised because sunlight falls toward the south from high solar altitudes. It is imperative to combine horizontal features with vertical shading in the east and west. However, in static shadowing conditions, the power generation efficiency can be increased by integrating a smart converter.

The suggested method is verified by modifying the temperature and irradiation levels while employing static shading in accordance with the real-time analysis. At $800\ W/$

m^2 and 25°C, respectively, the irradiance and temperature are kept constant. As there is constant shade throughout the day, there is steady illumination in this scenario. Figure 9, illustrates the suggested model's voltage and current values at full shade.

Under ideal circumstances, Figure 9, depicts the typical values for temperature and irradiance, which are $800 \, W/m^2$ and 25°C, respectively.
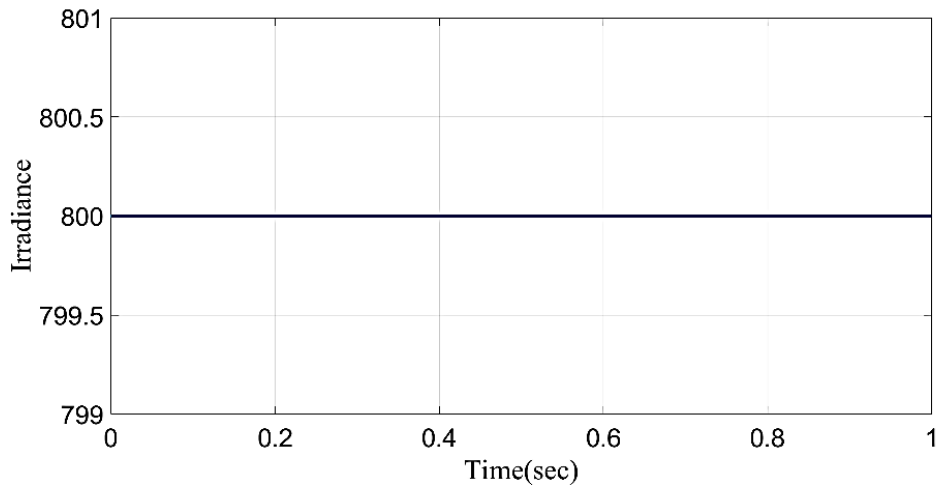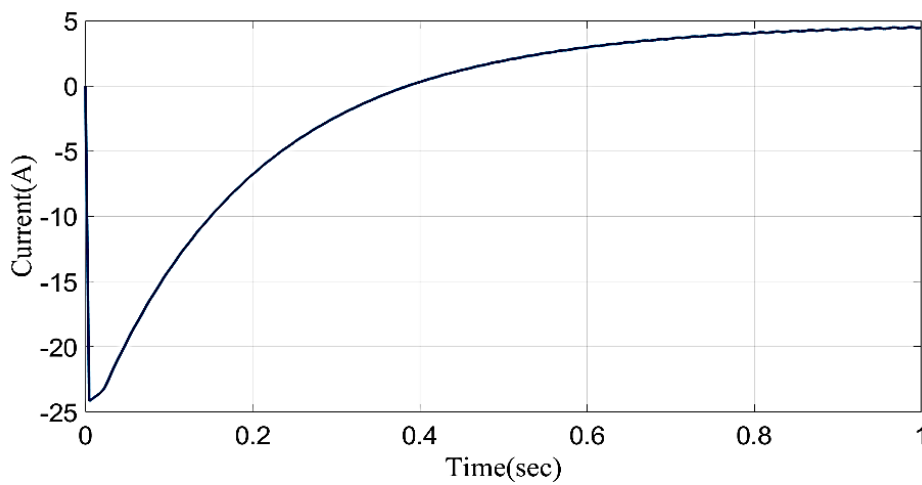

(a)
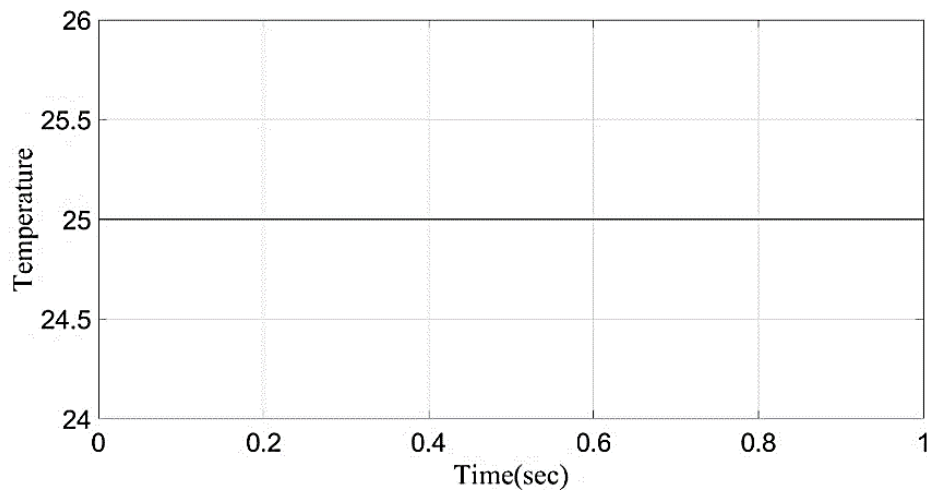
(b)

Figure 9. Investigation of PV under normal conditions: (a) irradiance (b) temperature.

(a)

(b)
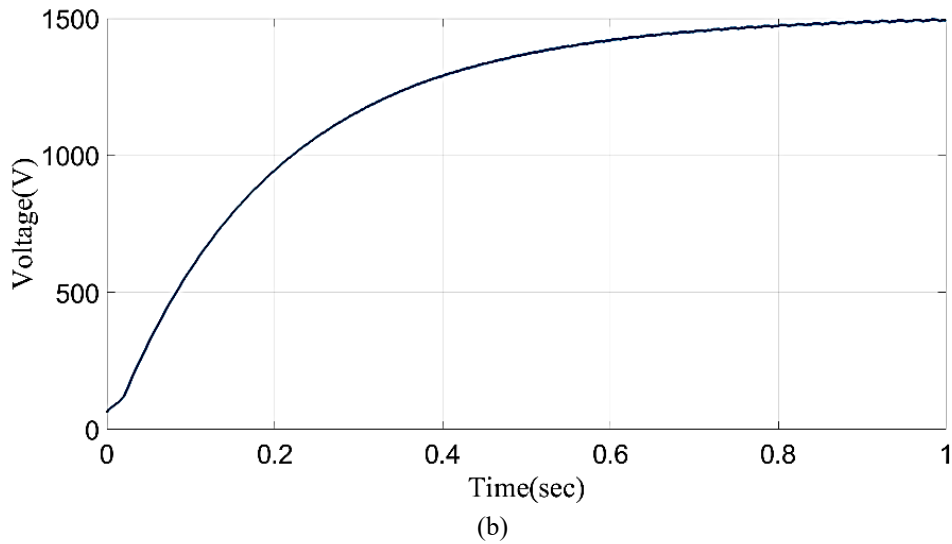
Figure 10. PV analysis at full shading with respect to (a) current and (b) voltage.

PV voltage and current under fully shading conditions are shown in Figure 10. The output in this case remained steady at 1500V and 4.9A since neither the temperature nor the amount of irradiation changed. At first, the current increases gradually until it reaches 4.7A after 0.9 seconds. After that, it flows continuously for a short while. It flowed steadily until the temperature and radiation changed from 25°C to $800\ W/m^2$, at which point it reached 4.9A in 0.9 seconds.

Figure 11, shows the power output from the PV. The amount of PV radiation is $800\ W/m^2$. At that moment, the output power is 0.6×10^4W. The optimal tracker provides a regular pulse for the boost converter during this time to provide the inverter with the generated constant power.
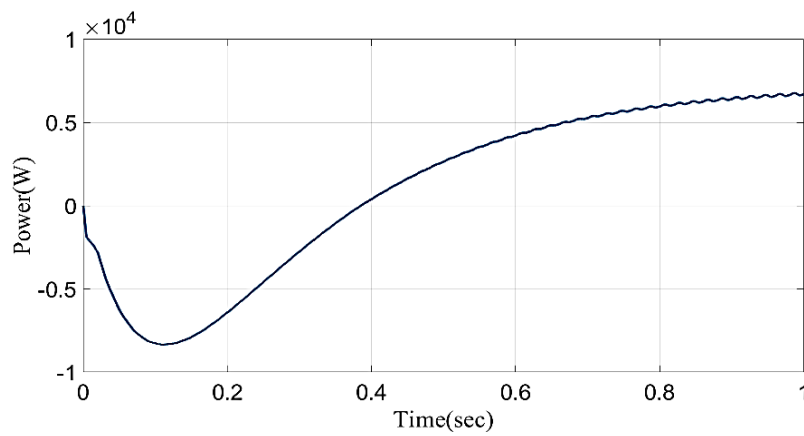
Figure 11. Analysis of PV power at fully shading condition.
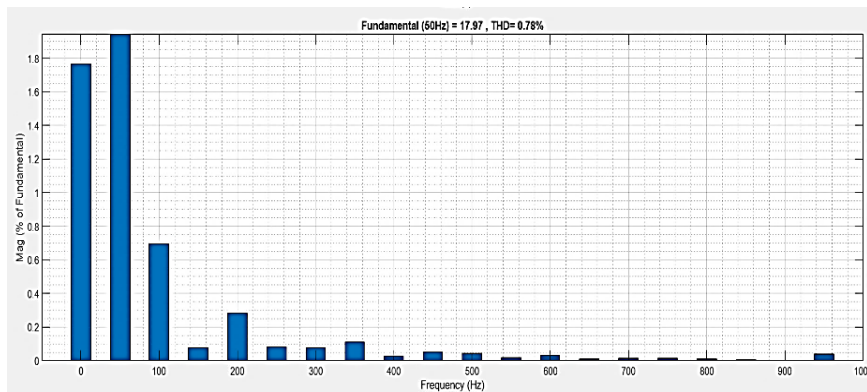
(a)
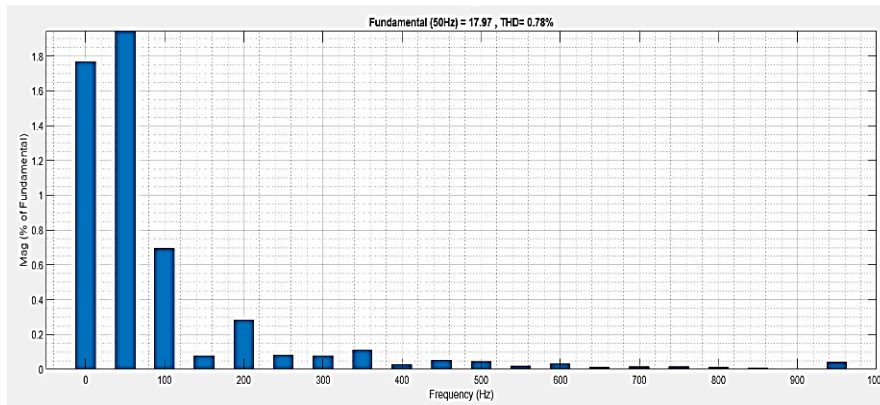
(b)

Figure 12. Analysis of harmonics (a) Voltage (b) Current THD at normal condition.

The Total Harmonic Distortion (THD) rating of the recommended converter is very low and the power factor is increased to 1 PF. In comparison with other methods now in use, this has a very low THD value and a very high PF. Figure 12, shows this obvious, with both the voltage and current THDs being 0.78% throughout this period.
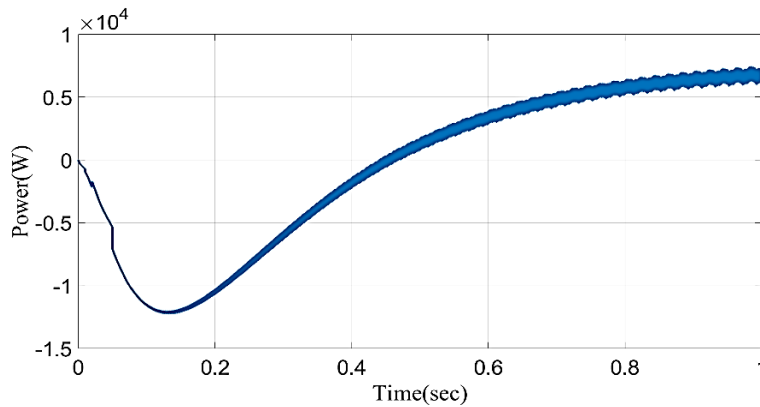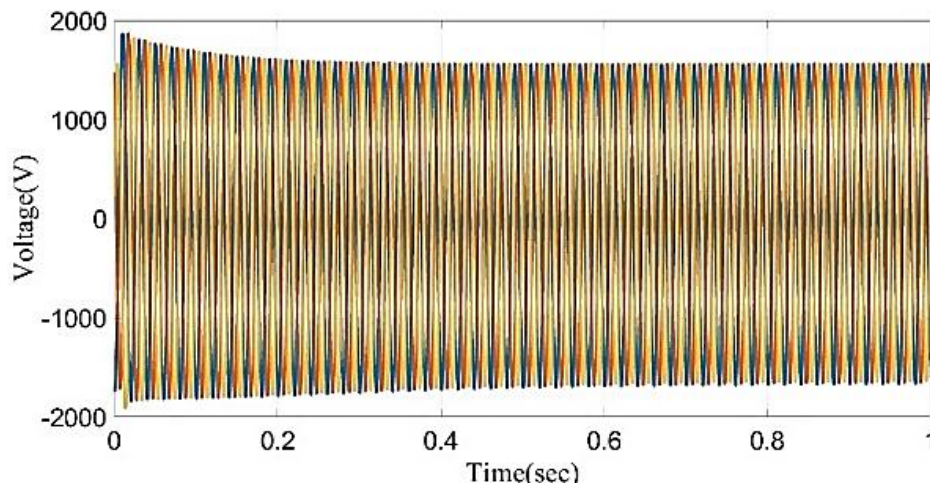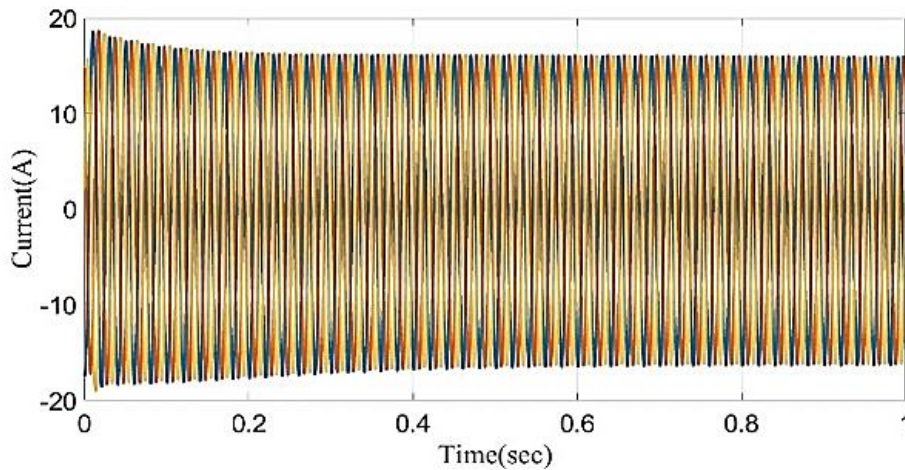

Figure 13. Analysis of DC-DC power at fully condition.

The main purpose of DC/DC power supply is to provide solar cells with a controlled voltage output throughout a range of operating conditions. The graphic demonstrates that under fully shading conditions, the DC/DC power remains constant at 0.6×10^4 is shown in Figure 13.


(a)

(b)

Figure 14. Evaluation of (a) load voltage and (b) load current at normal condition.

The term load refers to the power consumption of a device when it is used in a system. Figure 14, clearly shows how the load voltage and load current were studied. The load voltage is maintained at 1500V continuously for 0.4 to 1 second. It takes 0.2 to 1 second to maintain a 17A load current continuously in fully shading conditions.

3.4. Scenario 3: Partially shading conditions

One PV module is usually blocked out by surrounding structures, trees, birds in the sky, and partly overcast skies. As a result, there is inadequate solar insolation for one or more PV modules, which reduces current. Variations in solar radiation result in multiple power peaks in voltage and power characteristics. PV power and current are directly impacted by solar radiation. The PV voltage will be lowered or affected by more shade, which may be caused by outside variables like heat. The relationship between PV voltage and ambient temperature is inverse, and this is interpreted as a power loss. Moreover, this leads to the PV module functioning as a load and utilizing the power supplied by additional PV modules. This validates the suggested model's functionality under a dynamic shadow scenario.

The temperature and irradiance fluctuate throughout this time due to the erratic shadowing. By maintaining a constant temperature of 25°C and altering the irradiation to 850, 700, 900, and 1000W/m2, the proposed method examines the partially shading scenarios. During this period, there are variations in both the PV power and the MPP value as shown in Figure 15.
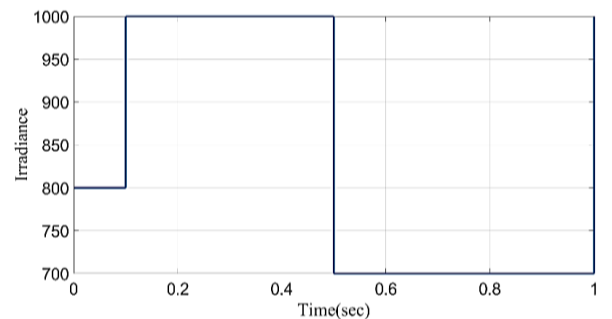
(a)
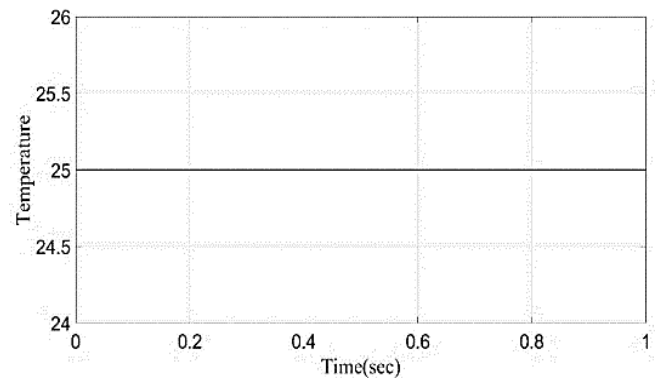
(b)

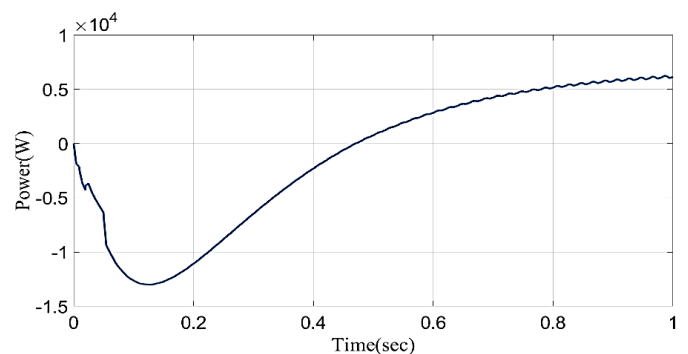Figure 15. PV analysis under fully shaded conditions (a) irradiance (b) temperature.

Figure 16. PV power analysis under totally shaded conditions.

Figure 16, shows the power output of the PV. PV radiation is present at a level of $850,700,900\ W/m^2$. The output power at this stage is 0.6×10^4. During this period, the boost converter obtains a regular pulse from the optimum tracker, which supplies the inverter with continuously generated power.
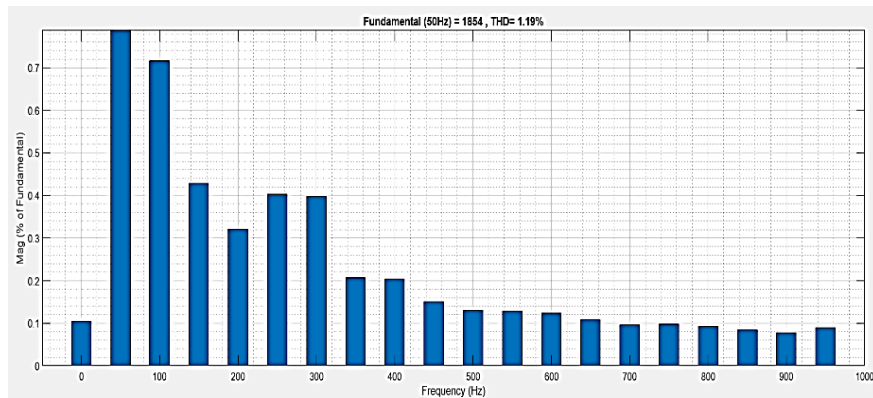
(a)
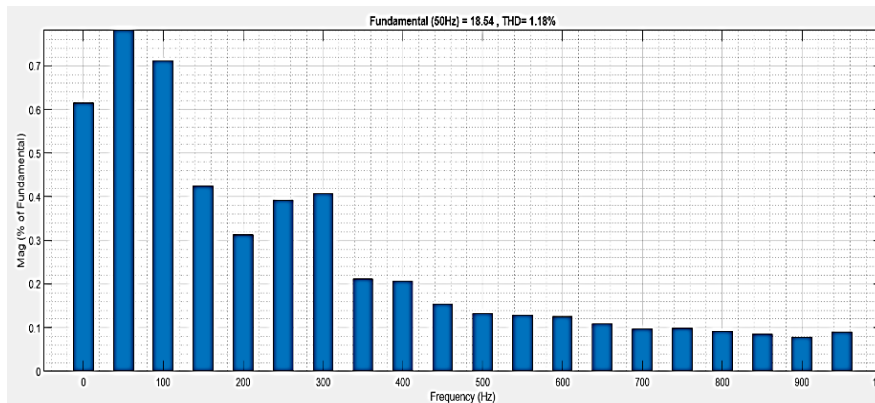
(b)

Figure 17. Harmonics analysis at full condition for (a) voltage and (b) current THD.

The recommended converter has an exceptionally low Total Harmonic Distortion (THD) rating and increases the power factor to 1 PF. Comparing this versus other methods currently in use, it has a very high PF and a very low THD. Figure 17, clearly illustrates the voltage THD of 1.18% and the current THD of 1.19% during this period.
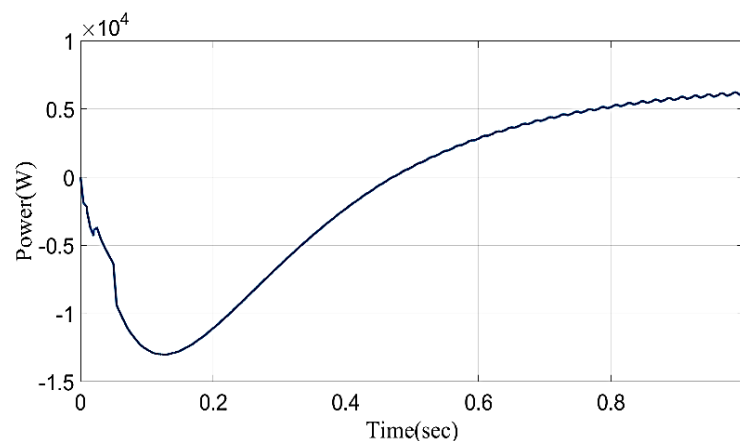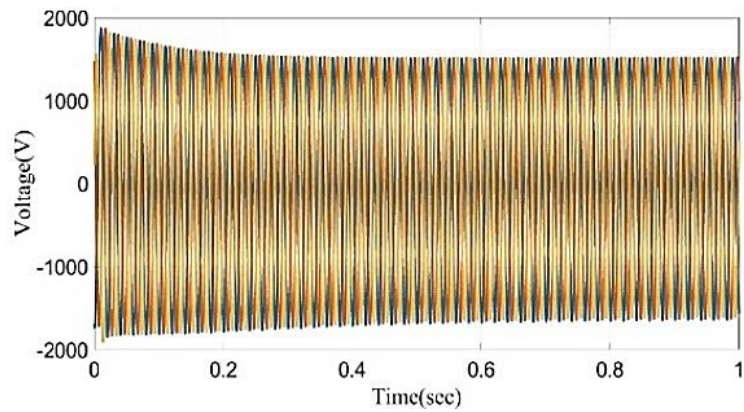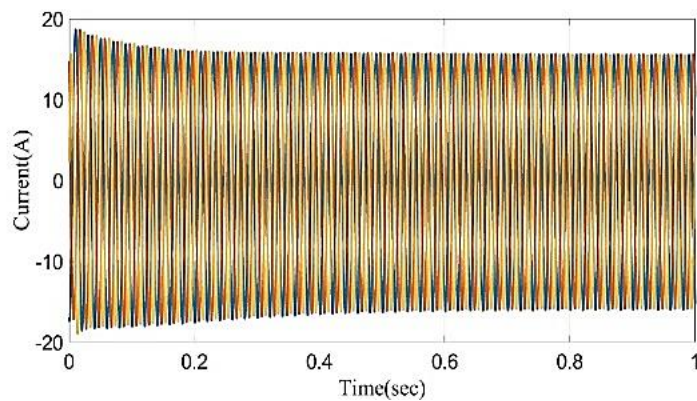

Figure 18. Analysis of DC-DC power at partial condition.

The key function of a DC/DC power supply is to provide solar cells with a controlled voltage output throughout a range of operating conditions. The Figure 18, demonstrates that under partially shading conditions, the DC/DC power remains constant at 0.6×10^4.

(a)

(b)

Figure 19. Analysis of (a) load voltage and (b) load current at normal condition.

A device's power consumption is referred to as its load when it is used in a system. The analysis of the load voltage and load current is clearly shown in Figure 19. The load voltage is kept constant at 1500V for 0.4 to 1 second. Maintaining a steady 17A load current consumes 0.2 to 1 seconds.

3.5. Optimal GAO tracker performance comparison

In this part, the overall outcome of the optimal DBN tracker is compared to traditional approaches by using GAO. The objective function is considered as the error value of each population.
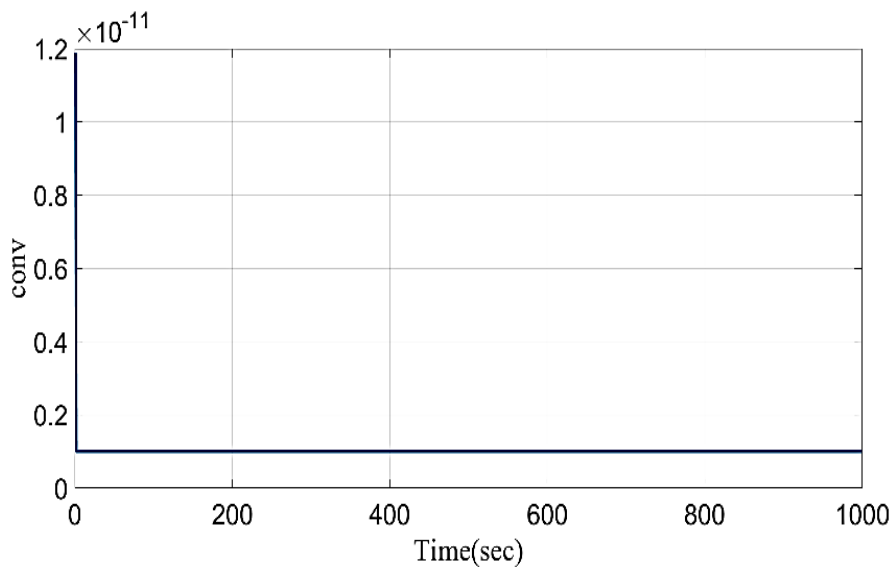

Figure 20. Analysis of convergence curve.

Figure 20, demonstrates the convergence curve of the proposed and conventional models. It demonstrates the proposed model have 1.0×10^{-11} error at 1st iteration which reduce to reach 0.1 error value at the 1st iteration. Thus, demonstrates the proposed model provides an effective optimal solution than the traditional models. In the following, the outcome of optimal DBN is compared to some traditional approaches like Feed Forward Neural Network (FFNN), Support Vector Matrix (SVM) and Multilayer Perceptron (MLP). The performance was a comparison of accuracy, precision, specificity, FPR, and error.
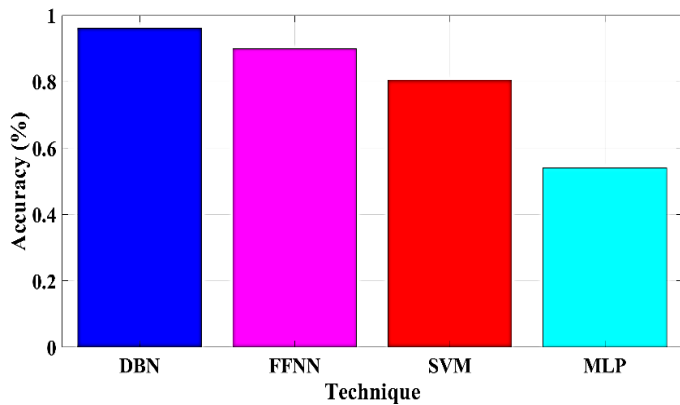

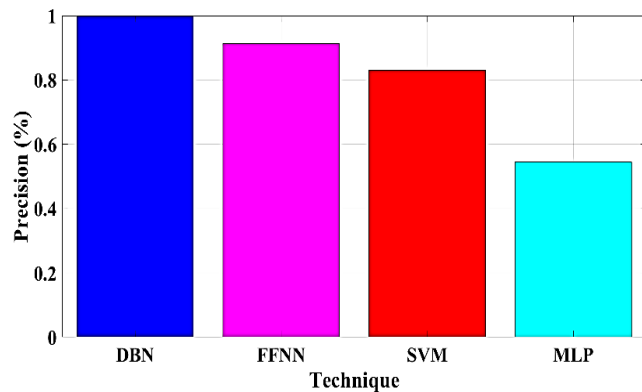Figure 21. Evaluation of accuracy.

Figure 22. Evaluation of precision.

As illustrated in Figure 21, the accuracy results were compared with a number of other current techniques such as FFNN, SVM, and MLP. FFNN has an accuracy rate of 90%, SVM is 80%, and MLP is 53%; the suggested technique has an accuracy rate of 96%. The desired and existing techniques precision is compared in Figure 22. The number of expected positive circumstances is the measure of precision. The preciseness of the proposed method was found to be 100%, in contrast to other current methods like FFNN, SVM, and MLP, which had respective precision values of 91%, 83%, and 54%.
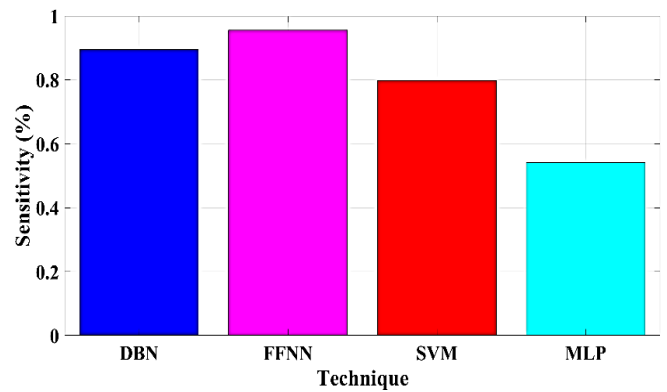
Figure 23. Evaluation of sensitivity.
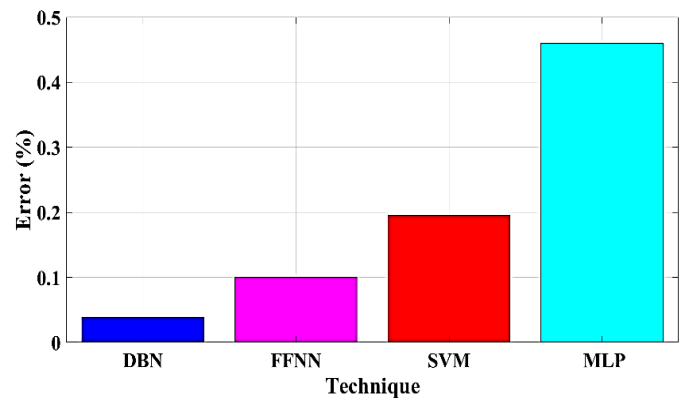
Figure 24. Evaluation of error.

The suggested and current approaches sensitivities are contrasted in Figure 23. The ratio between precisely positive and actually positive is known. The recommended method has a sensitivity of 89%, FFNN of 95%, SVM of 79%, and MLP of 54%. Next, a comparison is made between the error values of the suggested and current approaches. A system's error level indicates how many flaws or issues it has. Figure 24, presents an error comparison between the proposed and current methods. The error rates of the proposed method are 0.03%, 10%, 19%, and 46% for MLPs, FFNNs, and SVMs, respectively.

Figure 25. Evaluation of MCC.

Figure 26. Evaluation of F1_Score.

Figure 27. Evaluation of FPR.

Matthews's correlation coefficient (MCC) is a measure used to evaluate or quantify the discrepancy between expected and actual results. Figure 25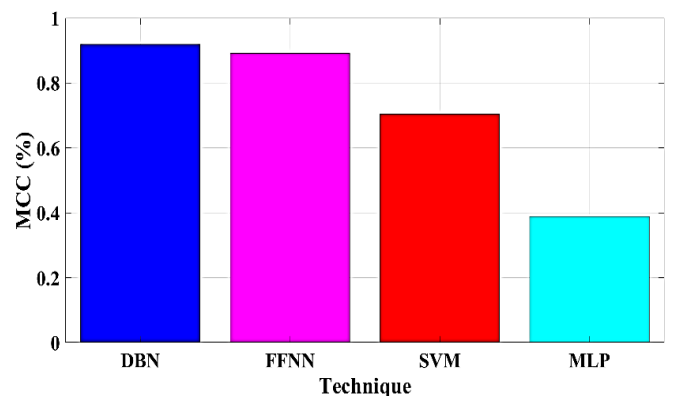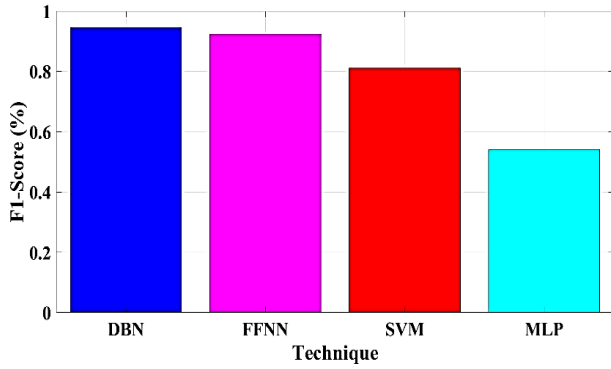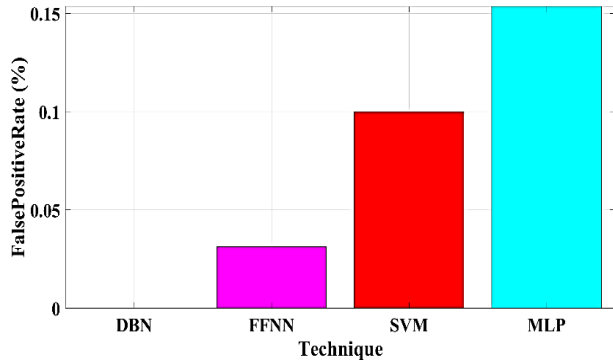, illustrates the values for the suggested MCC, FFNN, SVM, and MLP in the suggested approach, which are 91%, 89%, 70%, and 38%, respectively. The value of the F1 Score is next examined for both the suggested and the existing methods. A statistical study of the F1_ score reveals the binary types of the system and the correctness of the data collected. In Figure 26, the proposed and current F1 Scores are presented. The suggested technique's F1 Score values are 94%, 92% for MLP, 81% for SVM, and 54% for MLP. Figure 27, displays the False Positive Rate (FPR) for both planned and traditional approaches. The false positive rate for the suggested technique is 0%, FFNN is 0.03%, SSVM is 10%, and MLP is 15%, as shown in Figure 27.

3.6. Comparative analysis

To validate its performance, the detection efficacy of the proposed model is compared with several other existing approaches. Table 3, illustrates the MPPT tracking speed comparison between the proposed and current systems. It shows proposed GA-DBN provide 1ms tracking speed, FLC based P&O have 1.5ms tracking speed, ANFIS have 30ms tracking

speed and load current based MPPT have 80ms tracking speed [32].

Table 3. Tracking Speed Comparison.

MPPT Techniques	Tracking Speed (ms)
Proposed GA-DBN	$1ms$
FLC based P&O	$1.5ms$
ANFIS	$30ms$
P&O	$85ms$
Load current based MPPT	$80ms$

Table 4, shows proposed GA-DBN provide 99.8% efficiency, Artificial Neural Network- Back Propagation (ANN-BR) have 99.12% efficiency, Whale Optimization Algorithm (WOA) model have 91.51% efficiency, Grey Wolf Optimization (GWO) model have 99.5% efficiency and Particle Swarm Optimization (PSO) have 99.6% efficiency [33]. This comparison demonstrates that the suggested framework provides both high tracking efficiency and high tracking speed.

Table 4. Tracking Efficiency Comparison.

MPPT Techniques	Tracking Efficiency (%)
Proposed O-GRU	99.8
ANN-BR	99.9
WOA	99.9
GWO	99.5
PSO	99.6

The simulation results show that the recommended model is appropriate for all cases as it maintained system performance under unstable meteorological conditions by permitting the MPPT preserve an intelligent controller operational state while tracking the reference voltage.

4. Conclusion

The performance of the suggested optimum DBN-based converter integrated solar PV system was verified and it was effectively simulated under different weather situations. An FOPID-based DC-DC converter and a desirable DBN controller were presented. A conventional photovoltaic module was created based on the ranges, and its output fluctuated because of changes in sunlight and temperature intensity. Monitoring the PV model's temperature, current, voltage, and irradiance value resulted in the development of a real-time dataset. The DBN MPPT model, which tracks the maximum voltage of photovoltaic cells while analyzing temperature, voltage, current, and irradiance to generate a pulse signal for a DC-DC converter, was designed using this dataset as its basis. Consequently, an optimum DBN tracker system based on GAO was developed in

order to track the maximum power and produce a DC-DC converter pulse signal. Based on the created dataset and the Simulink model, the tracker system was created. Based on the acquired value, the converter was controlled by means of the proposed tracker. The FOPID controller's output was obtained by the DC-DC boost converter, which then used to generate switching pulses that transferred power to the load. The effectiveness of the proposed model was investigated using various natural scenario types, such as fully, partially, and normally shaded conditions. With a response time of under 1sec, the suggested model provides 99.8% efficiency and low harmonic values, such as the voltage THD of 0.78% and the current THD of 0.78%. The final simulation results show that the optimal MPPT controller with the FOPID controller that has been proposed is more efficient than the MPPT controller techniques that are already in use. In order to increase MPP tracking's training effectiveness and detection precision, future research will concentrate on developing a revolutionary artificial intelligence model. On another hand a modified layer is introduced in a neural network to make a fast process in sequence data.

References

1. Çeçen M, Yavuz C, Tırmıkçı CA, Sarıkaya S, Yanıkoğlu E. Analysis and evaluation of distributed photovoltaic generation in electrical energy production and related regulations of Turkey. Clean Technologies and Environmental Policy. 2022 Jan 7:1-6. https://doi.org/10.1007/s10098-021-02247-0

2. Lowe RJ, Drummond P. Solar, wind and logistic substitution in global energy supply to 2050–Barriers and implications. Renewable and Sustainable Energy Reviews. 2022 Jan 1;153:111720.

3. Aslam MS, Tiwari P, Pandey HM, Band SS. Observer-based control for a new stochastic maximum power point tracking for photovoltaic systems with networked control system. IEEE transactions on fuzzy systems. 2022 Oct 19;31(6):1870-84. https://doi.org/10.1109/TFUZZ.2022.3215797

4. Angadi S, Yaragatti UR, Suresh Y, Raju AB. System parameter based performance optimization of solar PV systems with perturbation based MPPT algorithms. Energies. 2021 Apr 5;14(7):2007. https://doi.org/10.3390/en14072007

5. Ibrahim NF, Mahmoud MM, Alnami H, Mbadjoun Wapet DE, Ardjoun SA, Mosaad MI, Hassan AM, Abdelfattah H. A new adaptive MPPT technique using an improved INC algorithm supported by fuzzy self-tuning controller for a grid-linked photovoltaic system. Plos one. 2023 Nov 3;18(11):e0293613.

6. Harrison A, Nfah EM, de Dieu Nguimfack Ndongmo J, Alombah NH. An Enhanced P&O MPPT Algorithm for PV Systems with Fast Dynamic and Steady-State Response under Real Irradiance and Temperature Conditions. International Journal of Photoenergy. 2022;2022(1):6009632.

7. Hichem L, Amar O, Leila M. Optimized ANN-fuzzy MPPT controller for a stand-alone PV system under fast-changing atmospheric conditions. Bulletin of Electrical Engineering and Informatics. 2023 Aug 1;12(4):1960-81. https://doi.org/10.11591/beei.v12i4.5099

8. Yahiaoui F, Chabour F, Guenounou O, Bajaj M, Hussain Bukhari SS, Shahzad Nazir M, Pushkarna M, Mbadjoun Wapet DE. An Experimental Testing of Optimized Fuzzy Logic-Based MPPT for a Standalone PV System Using Genetic Algorithms. Mathematical Problems in Engineering. 2023;2023(1):4176997.

9. Yilmaz M, Celikel R, Gundogdu A. Enhanced photovoltaic systems performance: anti-windup PI controller in ANN-based ARV MPPT method. IEEE Access. 2023 Jun 28. https://doi.org/10.1109/ACCESS.2023.3290316

10. Kaya CB, Kaya E, Gökkuş G. Training Neuro-Fuzzy by Using Meta-Heuristic Algorithms for MPPT. Computer Systems Science & Engineering. 2023 Apr 1;45(1). https://doi.org/10.32604/csse.2023.030598

11. Hassan, O. Bass, M. A. Masoum, An improved genetic algorithm based fractional open circuit voltage MPPT for solar PV systems," Energy Reports, 9, pp. 1535-1548, 2023. https://doi.org/10.1016/j.egyr.2022.12.088

12. Zand SJ, Mobayen S, Gul HZ, Molashahi H, Nasiri M, Fekih A. Optimized fuzzy controller based on cuckoo optimization algorithm for maximum power-point tracking of photovoltaic systems. IEEE Access. 2022 Jul 7;10:71699-716. https://doi.org/10.1109/ACCESS.2022.3184815

13. Abbass MJ, Lis R, Saleem F. The maximum power point tracking (MPPT) of a partially shaded PV array for optimization using the antlion algorithm. Energies. 2023 Mar 2;16(5):2380. https://doi.org/10.3390/en16052380

14. Chao KH, Li JY. Global maximum power point tracking of photovoltaic module arrays based on improved artificial bee colony algorithm. Electronics. 2022 May 14;11(10):1572. https://doi.org/10.3390/electronics11101572

15. Yang B, Wu S, Huang J, Guo Z, Wang J, Zhang Z, Xie R, Shu H, Jiang L. Salp swarm optimization algorithm based MPPT design for PV-TEG hybrid system under partial shading conditions. Energy Conversion and Management. 2023 Sep 15;292:117410.

16. Yaich M, Dhieb Y, Bouzguenda M, Ghariani M. Metaheuristic Optimization Algorithm of MPPT Controller for PV system application. InE3S Web of Conferences 2022 (Vol. 336, p. 00036). EDP Sciences. https://doi.org/10.1051/e3sconf/202233600036

17. Kumar GA, Shivashankar. Optimal power point tracking of solar and wind energy in a hybrid wind solar energy system. International Journal of Energy and Environmental Engineering. 2022 Mar;13(1):77-103. https://doi.org/10.1007/s40095-021-00399-9

18. Akram N, Khan L, Agha S, Hafeez K. Global maximum power point tracking of partially shaded PV system using advanced optimization techniques. Energies. 2022 May 31;15(11):4055. https://doi.org/10.3390/en15114055

19. Manna S, Singh DK, Akella AK, Kotb H, AboRas KM, Zawbaa HM, Kamel S. Design and implementation of a new adaptive MPPT controller for solar PV systems. Energy Reports. 2023 Dec 1;9:1818-29. https://doi.org/10.1016/j.egyr.2022.12.152

20. Manoharan P, Subramaniam U, Babu TS, Padmanaban S, Holm-Nielsen JB, Mitolo M, Ravichandran S. Improved perturb and observation maximum power point tracking technique for solar photovoltaic power generation systems. IEEE Systems Journal. 2020 Jul 13;15(2):3024-35. https://doi.org/10.1109/JSYST.2020.3003255

21. Xu L, Cheng R, Yang J. A new MPPT technique for fast and efficient tracking under fast varying solar irradiation and load resistance. International Journal of Photoenergy. 2020;2020(1):6535372.

22. Obukhov S, Ibrahim A, Diab AA, Al-Sumaiti AS, Aboelsaud R. Optimal performance of dynamic particle swarm optimization based maximum power trackers for stand-alone PV system under partial shading conditions. IEEE Access. 2020 Jan 13;8:20770-85. https://doi.org/10.1109/ACCESS.2020.2966430

23. Chalok KH, Tajuddin MF, Babu TS, Ayob SM, Sutikno T. Optimal extraction of photovoltaic energy using fuzzy logic control for maximum power point tracking technique. International Journal of Power Electronics and Drive Systems. 2020 Sep 1;11(3):1628. https://doi.org/10.11591/ijpeds.v11.i3.pp1628-1639

24. Patra B, Nema P, Khan MZ, Khan O. Optimization of solar energy using MPPT techniques and industry 4.0 modelling. Sustainable Operations and Computers. 2023 Jan 1;4:22-8. https://doi.org/10.1016/j.susoc.2022.10.001

25. González-Castaño C, Restrepo C, Revelo-Fuelagán J, Lorente-Leyva LL, Peluffo-Ordóñez DH. A fast-tracking hybrid mppt based on surface-based polynomial fitting and p&o methods for solar pv under partial shaded conditions. Mathematics. 2021 Oct 28;9(21):2732. https://doi.org/10.3390/math9212732

26. Dagal I, Akın B, Akboy E. Improved salp swarm algorithm based on particle swarm optimization for maximum power point tracking of optimal photovoltaic systems. International journal of energy research. 2022 Jun 10;46(7):8742-59. https://doi.org/10.1002/er.7753

27. Sivakumar, Narendiran, Jaisiva Selvaraj, Karthika Jayaprakash, and Kinde Anlay Fante. "Optimized DBN-based control scheme for power quality enhancement in a microgrid cluster connected with renewable energy system." *IET Renewable Power Generation* 18, no. 12 (2024): 1926-1947. https://doi.org/10.1049/rpg2.13058

28. Jamal, Jamal, Ilyas Mansur, Adam Rasid, Musrady Mulyadi, Muhammad Dihyah Marwan, and Marwan Marwan. "Evaluating the shading effect of photovoltaic panels to optimize the performance ratio of a solar power system." *Results in Engineering* 21 (2024): 101878.

29. Hussaian Basha, Chakarajamula, Madhu Palati, C. Dhanamjayulu, S. M. Muyeen, and Prashanth Venkatareddy. "A novel on design and implementation of hybrid MPPT controllers for solar PV systems under various partial shading conditions." *Scientific Reports* 14, no. 1 (2024): 1609. https://doi.org/10.1038/s41598-023-49278-9

30. Mai, Chunliang, Lixin Zhang, Xuewei Chao, Xue Hu, Xiaozhao Wei, and Jing Li. "A novel MPPT technology based on dung beetle optimization algorithm for PV systems under complex partial shade conditions." *Scientific Reports* 14, no. 1 (2024): 6471. https://doi.org/10.1038/s41598-024-57268-8

31. Naser, Abdulbari Talib, Karam Khairullah Mohammed, Nur Fadilah Ab Aziz, Karmila binti Kamil, and Saad Mekhilef. "Improved coot optimizer algorithm-based MPPT for PV systems under complex partial shading conditions and load variation." *Energy Conversion and Management: X* 22 (2024): 100565.

32. Podder AK, Roy NK, Pota HR. MPPT methods for solar PV systems: a critical review based on tracking nature. IET Renewable Power

Generation. 2019 Jul;13(10):1615-32. https://doi.org/10.1049/iet-rpg.2018.5946

33. Ncir N, El Akchioui N. An intelligent improvement based on a novel configuration of artificial neural network model to track the maximum power point of a photovoltaic panel. Journal of Control, Automation and Electrical Systems. 2023 Apr;34(2):363-75. https://doi.org/10.1007/s40313-022-00972-5